

# EHRFL: Federated Learning Framework for Heterogeneous EHRs and Precision-guided Selection of Participating Clients

Jiyoun Kim<sup>1</sup>

JIYOUN.KIM@KAIST.AC.KR

Junu Kim<sup>1</sup>

KJUNE0322@KAIST.AC.KR

Kyunghoon Hur<sup>1</sup>

PACESUN@KAIST.AC.KR

Edward Choi<sup>1</sup>

EDWARDCHOI@KAIST.AC.KR

<sup>1</sup> *Korea Advanced Institute of Science and Technology (KAIST)*

## Abstract

In this study, we provide solutions to two practical yet overlooked scenarios in federated learning for electronic health records (EHRs): firstly, we introduce EHRFL, a framework that facilitates federated learning across healthcare institutions with distinct medical coding systems and database schemas using text-based linearization of EHRs. Secondly, we focus on a scenario where a single healthcare institution initiates federated learning to build a model tailored for itself, in which the number of clients must be optimized in order to reduce expenses incurred by the host. For selecting participating clients, we present a novel precision-based method, leveraging data latents to identify suitable participants for the institution. Our empirical results show that EHRFL effectively enables federated learning across hospitals with different EHR systems. Furthermore, our results demonstrate the efficacy of our precision-based method in selecting reduced number of participating clients without compromising model performance, resulting in lower operational costs when constructing institution-specific models. We believe this work lays a foundation for the broader adoption of federated learning on EHRs.<sup>1</sup>

## 1. Introduction

In the contemporary healthcare environment, there is an exponential accumulation of electronic health records (EHRs), driven by daily patient interactions and clinical activities. Models leveraging extensive longitudinal EHRs demonstrate enhanced capability for accurate prediction of patient status across a variety of predictive tasks (Rajkomar et al., 2018; Amirahmadi et al., 2023).

With the evolving landscape of machine learning, there is a growing necessity for models to be trained on extensive data (Choi et al., 2016; Yang et al., 2022), making it insufficient to solely utilize data from a single medical institution (Dash et al., 2019). Traditional approaches for modeling across multiple datasets have relied on centralized learning, wherein raw data is aggregated in a central repository for the purpose of model training. However, the constraints imposed by patient privacy concerns through data aggregation preclude the feasibility of centralized learning, thereby underscoring the imperative for federated learning in healthcare (Rieke et al., 2020; Rahman et al., 2023).

---

1. Code is available at <https://github.com/ji-young-kim/EHRFL>

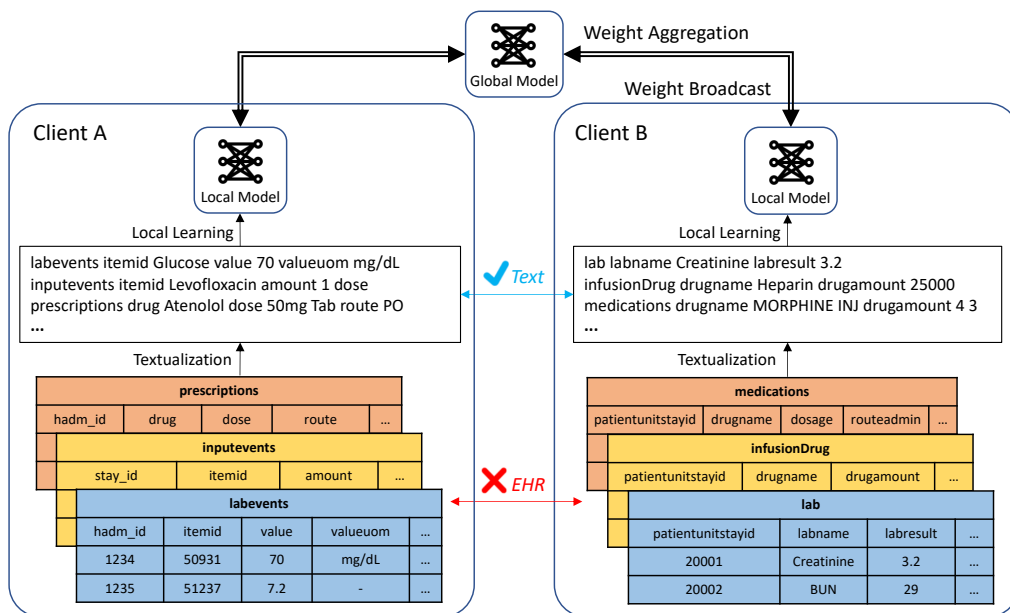


Figure 1: Visualization of EHRFL, our framework which enables federated learning across heterogeneous EHR systems. By transforming each EHR event into linearized text-based representations, local models of different healthcare institutions are trained in a unified data format. The local model and global model weights are aggregated and broadcasted respectively for federated learning.

Federated learning (McMahan et al., 2017) is a decentralized training method that collaboratively updates a global model through the integration of locally trained models. This approach circumvents the need for central data storage inherent in traditional centralized training by only sharing model weights instead. The method facilitates the harness of rich, diverse data while concurrently adhering to strict compliance with data privacy norms.

However, two realistic yet overlooked scenarios exist in the context of EHR federated learning, which we address and provide solutions for.

The first scenario pertains to federated learning on heterogeneous EHR systems. Specifically, different healthcare providers utilize disparate medical code systems (i.e., ICD-9, ICD-10) and different database schemas for storing patient data. To enable federated learning across distinct EHRs, it is necessary to integrate these disparate code systems and schemas into a unified format for compatible modeling. While one potential solution involves converting each EHR system into a Common Data Model (CDM) format (Rajkomar et al., 2018), this approach has been unexplored in prior federated learning studies due to the time-consuming and costly nature of constructing CDMs. Instead, existing EHR federated learning research predominantly focus on establishing experimental setups within homogeneous client settings by partitioning data within the same hospital or database (Lee and Shin, 2020; Vaid et al., 2021; Dang et al., 2022; Rajendran et al., 2023). However, such an approach does not accurately emulate real-world scenarios of federated learning applied across hospitals, which often have different medical coding systems and database schemas. This necessitates a framework for federated learning on heterogeneous EHRs.

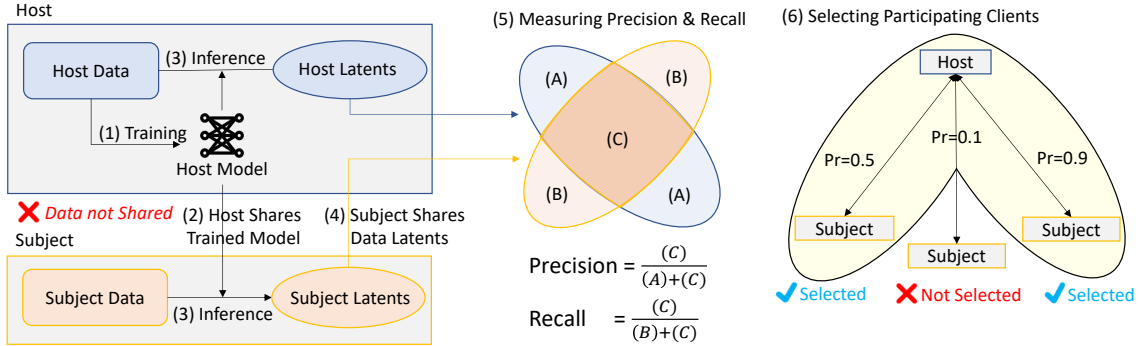


Figure 2: Visualization of our precision-based method for selecting participating clients. (Left) The host and subjects each extract data latents from their own data respectively, using a common model trained by the host. Each subject sends their latents to the host. (Middle) The host computes precision (and recall) of each subject. (Right) Based on the precision score (Pr), the host selects federated learning participants by excluding clients with low precision values.

The second scenario centers on a potentially practical situation where a single healthcare institution initiates federated learning to develop a model tailored specifically for its own use. In contrast to existing federated learning research which predominantly focus on collaboratively creating a global model for multiple clients (Zhang et al., 2021; Wen et al., 2023), one conceivable scenario involves a hospital assembling clients to engage in federated learning aimed at creating a model for itself. This approach incurs costs for the host (i.e., initiating institution), including compensations for clients’ participation (i.e., data usage payments) and the construction of a network infrastructure to facilitate the involvement of multiple participants. As the number of clients increase, so do the costs incurred by the host, including data usage payments to each client and infrastructure development (Majeed et al., 2022). This underscores the importance of optimizing the number of participating clients to reduce expenses. Furthermore, the inclusion of certain clients may not affect, or could potentially degrade, the model’s performance from the perspective of the host institution. Thus, in order to eliminate unnecessary costs for the host, it is crucial to identify and exclude such clients from the federated process.

As a solution for the first scenario, we incorporate the methodology of Hur et al. (2023) into federated learning, and propose a Federated Learning framework for heterogeneous Electronic Health Records (EHRFL). In their study, Hur et al. (2023) introduced a method for EHR modeling that addresses the issue of code and database schema heterogeneity of EHRs. The method involves converting medical codes and schemas into a unified text-based representation, facilitating EHR modeling of distinct healthcare systems. However, their focus was exclusively on centralized learning, which encounter significant limitations in practical application due to patient privacy concerns as mentioned above. By integrating the method into federated learning, our framework eliminates the requirement for intricate mapping of medical codes and database schemas, thereby facilitating collaborative federated learning across different EHR systems.

To address the second scenario, we propose a precision-based method to exclude participating clients that either negligibly contribute to or negatively affect federated learning

performance in the perspective of a single healthcare institution, for cost reduction incurred by the host. Recently, in the domain of computer vision, [Kynkäänniemi et al. \(2019\)](#) proposed a method for assessing the quality of generated images in relation to the original image by using precision and recall of generated and original image latents. Inspired by this method, we adapt it to the federated learning domain to measure data similarities between clients by utilizing data latents. With our proposed precision-based approach, the host eliminates clients with low precision scores among all candidate clients for federated learning participation, thereby reducing the number of participating clients while maintaining model performance for the host.

Through extensive experiments on multiple open-source datasets with different medical codes and schemas, we show that our EHRFL framework, for the first time, enables federated learning across hospitals with varying medical codes and schemas. Furthermore, our experiments reveal that there is correlation between latent-based precision scores and performance difference between the host performance on federated learning and that of the single-source model trained exclusively on the host’s data. This relationship is consistently observed across various cohort sizes settings. Additionally, applying our precision-based method for selecting clients involved in federated learning can enable the participation of fewer clients without performance trade-off, which leads to reduced operational costs. We believe our work establishes foundational groundwork for the widespread application in multiple scenarios of federated learning on electronic health records.

### **Generalizable Insights about Machine Learning in the Context of Healthcare**

In healthcare, the diversity in medical code systems and database schemas among different hospitals poses a significant challenge for federated learning. While previous research often construct clients within homogeneous datasets or databases, such approaches do not capture the complexities of real-world scenarios. To bridge this gap, we introduce the EHRFL framework, which enables federated learning across diverse EHR systems by leveraging text-based linearization of EHRs. Our empirical evaluations demonstrate, for the first time to our knowledge, the efficacy and practicality of federated learning on heterogeneous EHR systems.

Moreover, in practical healthcare scenarios, healthcare institutions may seek to develop a model tailored for its own use. However, more clients involved in the federated learning process inevitably leads to increased costs. Thus, there is a critical need for strategies that minimize client involvement, without model performance trade-off. To address this challenge, we present a novel precision-based method for selecting participating clients. Our experimental analysis confirms the viability of reducing participant numbers while sustaining model performance, particularly when suitable clients are selected. Furthermore, our results highlight the efficacy of our precision-based approach compared to various baselines, validating that our method can effectively reduce the number of participating clients while preserving the performance level that can be achieved when all clients are involved.

## **2. Related Work**

**Federated Learning on EHRs** In recent years, EHR federated learning has been extensively explored, primarily due to its capability to utilize data from multiple institutions

without directly sharing patient data (Lee and Shin, 2020; Vaid et al., 2021; Dang et al., 2022; Rajendran et al., 2023). These studies perform various predictive tasks on open-source datasets such as Johnson et al. (2016); Pollard et al. (2018) or that of proprietary EHR systems. However, a common limitation of existing studies lies in the oversimplified construction of clients, often achieved by partitioning a single dataset or database into multiple clients to simulate a federated learning setting. This simplification is primarily attributed to the challenges associated with addressing code and schema heterogeneity across diverse datasets, leading to a disparity between experimental settings and practical scenarios.

**Client Distance Measurement in Federated Learning** Aligned yet distinct from our objectives, there exists prior research on measuring distances between clients in the context of federated learning. For instance, Huang et al. (2019); Elhussein and Gürsoy (2023) have introduced clustered federated learning methods for grouping clients based on similarity, enabling the training of distinct models for each cluster. Specifically, Huang et al. (2019) implemented K-means clustering (euclidean distance-based) on patient representation vectors from each client, derived from a common pre-trained autoencoder model. Similarly, Elhussein and Gürsoy (2023) employed cosine similarity to create matrices that represent client similarities, using patient representation vectors extracted in the same manner. Unlike these approaches, our work introduces a precision-based method to compute the distance between clients, aiming to identify clients for exclusion when building a model for a single host.

### 3. Federated Learning Framework for Heterogeneous EHRs

In this section, we introduce EHRFL, designed to facilitate federated learning across disparate EHRs with varied medical codes and database schemas. An overview of our framework is shown in Figure 1. Our framework consists of two key components: (1) Text-based EHR Modeling and (2) Federated Learning. For the first component, we employ the methodologies delineated by Hur et al. (2023), and subsequently integrate these strategies with federated learning.

#### 3.1. Text-based EHR Modeling

**Structure of EHR** For each patient  $P$ , EHRs exhibit a hierarchical structure comprising two levels: event level and feature level. The medical history of Patient  $P$  is represented through a series of discrete medical events, denoted as  $m_1, m_2, \dots, m_i, \dots$ , where  $i$  indexes each event. Each event  $m_i$  is characterized by a specific event type  $e_i$ , such as ‘labevents’, ‘inpuvents’, and ‘prescriptions’. Each event  $m_i$  also comprises a set of feature pairs, where each pair consists of a feature name and its corresponding value  $(n_{ij}, v_{ij})$  within the context of  $m_i$ . Examples of feature pairs  $(n_{ij}, v_{ij})$  include (‘itemid’, 50931), (‘value’, 70), and (‘valueuom’, ‘mg/dL’). Given that the medical code systems, event types, and feature names may differ across healthcare institutions, it is essential to transform this data into a compatible format to enable federated learning on EHRs.

**Text-based EHR Linearization** In order to convert EHRs into a compatible format, we represent each event into a text-based format, by concatenating the event type and feature pairs, following the method of Hur et al. (2023). If  $v_{ij}$  denotes a medical code, it is replaced with its corresponding medical text, denoted as  $v'_{ij}$ . For example, medical code

50931 can be converted to 'Glucose'. If  $v_{ij}$  is not a medical code, it retains its original value, which we also denote as  $v'_{ij}$ . The text-based event representation  $r_i$  for each  $m_i$  is as follows:

$$r_i = (e_i \oplus n_{i1} \oplus v'_{i1} \oplus n_{i2} \oplus v'_{i2} \dots)$$

, where  $\oplus$  denotes concatenation.

**Modeling of EHRs.** To capture the hierarchical structure inherent in EHRs, we adopt the strategy of Hur et al. (2023), and encode the event representations of each patient into event vectors, which are then aggregated to form a patient representation vector. Specifically, the linearized event representation  $r_i$  is tokenized and then processed through an event encoder model (i.e., *EventEncoder*) to generate the corresponding event vector  $z_i$ . We use a 2-layer Transformer encoder (Vaswani et al., 2017) for *EventEncoder*, consistent with Hur et al. (2023). When  $Z$  represents the set of event vectors ( $z_1, z_2, \dots, z_i, \dots$ ) and  $R$  represents the event representations ( $r_1, r_2, \dots, r_i, \dots$ ) for a patient, the encoding process is specified as follows:

$$Z = \text{EventEncoder}(\text{Tokenize}(R))$$

The event vectors  $Z$  of each patient are subsequently aggregated using an aggregator model (i.e., *Aggregator*), wherein the vectors undergo a second encoding process and then are averaged to produce a patient latent vector  $l$ . *Aggregator* employs a 2-layer Transformer encoder (Vaswani et al., 2017), concluding with mean pooling to integrate the event vectors.

$$l = \text{Aggregator}(Z)$$

Subsequently, the patient vectors  $L$  (comprising  $l_1, l_2, \dots$ ) are trained to minimize the sum of the prediction loss (e.g., cross-entropy loss) across all tasks within the healthcare institution.

### 3.2. Federated Learning

With the above text-based EHR modeling method, it is possible to collaboratively train a federated learning model for the host with multiple healthcare institutions of distinct EHR systems involved. The overall federated learning process is specified below.

1. *Local Model Training:* Each participating client  $C_k$  trains a local model  $M_k$  on its dataset  $D_k$ , to minimize prediction loss.

$$M_k^{new} = \text{LocalTrain}(M_k, D_k)$$

where  $M_k^{new}$  represents the updated local model for client  $C_k$ .

2. *Model Aggregation:* Post local training, local models of each client are sent to a central server. The server aggregates the local model weights of clients to update the global

model  $M_{global}$ .

$$M_{global}^{new} = w_k \sum_{k=1}^N M_k^{new}$$

where  $N$  is the number of clients and  $w_k$  is the aggregation weight for client  $C_k$ . The aggregation weight for each client is a positive value which sums up to 1 across all participating clients.

3. *Global Model Broadcasting*: The updated global model  $M_{global}^{new}$  is then sent back to each client for the next communication round of local training.

This process is repeated until the model converges based on the early stopping criterion, or until when the maximum predefined number of communication rounds is reached.

#### 4. Precision-guided Selection of Participating Clients

In this section, we introduce our precision-based method of identifying clients to exclude from the federated learning process when constructing a model for a single healthcare institution. We refer to *host* as the client initiating federated learning, and *subject* as the candidate client considered for participation alongside the host. Figure 2 shows an overview of our method.

First, the host initiates training a single model on its own training data with the modeling method in Section 3.1. This step is taken to develop a common model for extracting latent representations of both host and subject data. Second, the host transmits the trained model weights to each candidate subject. Third, the subjects and the host each independently process their data through the trained host model to extract latent representations. We define  $L_s$  as the patient latent vectors of a single candidate subject, and  $L_h$  as that of the host. Fourth, the candidate subjects each share their latent  $L_s$  to the host. Fifth, the host computes precision and recall of each subject using distribution of  $L_s$  and  $L_h$  for each subject. Specifically, precision is measured by identifying the overlapping sections of the distributions of  $L_h$  and  $L_s$  within the distribution of  $L_h$ , while recall is determined by the overlap of both distributions within the distribution of  $L_s$ . As shown in Figure 2, when the distribution of  $L_h$  is (A) + (C), that of  $L_s$  is (B) + (C), and the overlapping distribution is (C), precision is defined as follows:

$$Precision = \frac{(C)}{(A) + (C)}$$

Recall is defined as follows:

$$Recall = \frac{(C)}{(B) + (C)}$$

Sixth, based on the precision scores of the candidate subjects, the host identifies subjects with low precision scores and excludes them from the federated learning process. This exclusion can be performed by selecting the top  $k$  subjects with the lowest precision scores.

Due to the complexity of measuring latent distributions, we compute precision and recall of latents using the K-Nearest Neighbors (KNN) algorithm, as described in [Kynkäänniemi et al. \(2019\)](#). Specifically, given the latent of a single client ( $L_s$  for a subject and  $L_h$  for the host), we establish the latent manifold by creating a hypersphere around each data point within the latent, where the radius is set to the distance to its k-th nearest data point. Precision is then computed by dividing the number of data points in  $L_s$  within the manifold of  $L_h$  by the total number of vectors in  $L_h$ . Similarly, recall is computed by dividing the number of data points in  $L_h$  within the manifold of  $L_s$  by the total number of vectors in  $L_s$ .

## 5. Experiments & Results

In this section, we conduct three experiments. The first experiment focuses on federated learning across multiple medical institutions with differing medical codes and database schemas. This experiment aims to assess the efficacy of EHRFL when conducting federated learning on heterogeneous EHR systems. The second experiment investigates the relationship between precision and model performance difference across diverse host-subject pairs. Here, model performance difference refers to the difference in host performance when performing federated learning with a subject involved, compared to the performance of a single-source model built solely upon the host’s data. Positive correlation between precision and model performance difference would justify the exclusion of clients with low precision scores to prevent negligible or adverse impact on model performance. Building upon the findings obtained in the second experiment, the third experiment applies the precision-based method to the first experiment, for identifying clients to exclude from the federated learning process, in the perspective of each host. The ultimate goal is to eliminate unnecessary costs for the host by reducing the number of participating clients without compromising the model’s performance.

### 5.1. Datasets

For our experiments, we utilize three open-sourced EHR datasets: MIMIC-III ([Johnson et al., 2016](#)), MIMIC-IV ([Johnson et al., 2020](#)), and eICU ([Pollard et al., 2018](#)), which all consist of patient ICU data. MIMIC-III and MIMIC-IV are derived from the same medical institution but cover different time periods and differ in database schemas (MIMIC-III spans 2001-2012, MIMIC-IV covers 2008-2019). The eICU dataset includes data from multiple hospitals across the United States. To accommodate the differences in database systems within MIMIC-III (CareVue and MetaVision databases), we split it into two separate clients: MIMIC-III-CV (CareVue) and MIMIC-III-MV (MetaVision). This division is necessitated by the variations in their schemas and the distinct periods covered by each system (CareVue from 2001-2008 and MetaVision from 2009-2012). For MIMIC-IV, we exclude data from the overlapping period of 2008-2012 with MIMIC-III, in order to ensure no temporal overlap between the two datasets. Given the relatively small size of each hospital data within eICU dataset compared to MIMIC, we constructed two clients to reflect geographical heterogeneity: eICU-South and eICU-West. This division ensures that there is no geographical overlap with the MIMIC datasets, which originate from the Northeast region. To summarize, we construct a total of 5 clients from 4 different EHR database systems across 3 different



geographical regions, featuring heterogeneous demographics and label distributions, listed in Appendix B.

## 5.2. Experimental Settings

Our cohorts include patients admitted to the ICU over the age of 18, with a minimum stay of 12 hours. We use the first ICU stay data for each hospital admission. The initial 12 hours of data within each ICU stay are utilized to generate predictions regarding patient outcomes in the subsequent 24 hours. We conduct our experiments on 12 clinical tasks, previously outlined by Hur et al. (2023). The task definitions are available in Appendix A. Consistent with Hur et al. (2023), we adopt a multi-task learning approach, and train our model on the 12 clinical prediction tasks simultaneously.

For federated learning, we experiment on four widely used algorithms:

- FedAvg (McMahan et al., 2017): a cornerstone federated learning algorithm that aggregates model updates by averaging weights of locally trained models.
- FedProx (Li et al., 2020): extends FedAvg by incorporating a proximal term to the local training objective, which aims to reduce divergence in local updates caused by the non-IID (Non-Independent and Identically Distributed) issue of client data (Li et al., 2022).
- FedBN (Li et al., 2021): maintains separate batch normalization parameters for each client during the aggregation process, which deals with the non-IID challenge in federated learning.
- FedPxN (Hwang et al., 2023): integrates FedProx’s proximal regularization with FedBN’s client-specific normalization, in order to mitigate the non-IID issue by harnessing both methods.

We set the maximum number of communication rounds to 300, with each round consisting of a single local epoch. This aligns to the hyperparameter settings of Hwang et al. (2023), who observe that reducing the number of local training epochs while increasing the frequency of communication rounds generally leads to improved overall performance in federated learning. Additionally, following their settings, the final model for the host is selected based on the model with highest performance on the host’s validation set. All experiments are run across three random seeds, each featuring different data splits and model initializations.

For each experiment, we used four NVIDIA GeForce 3090 GPUs, each with 24G of RAM, and corresponding Cuda version of 11.4. The training duration for each experiment below ranges from 2 hours to a maximum of 2 days respectively.

## 5.3. Federated Learning across Heterogeneous EHRs

In this section, we present the federated learning results using our EHRFL framework, incorporating five distinct clients with heterogeneous EHRs, specifically MIMIC-III-CV, MIMIC-III-MV, MIMIC-IV, eICU-South, and eICU-West mentioned above. To the best

Method	MIMIC-III-CV	MIMIC-III-MV	MIMIC-IV	eICU-South	eICU-West
Single	0.799±0.004	0.802±0.004	0.814±0.007	0.775±0.005	0.770±0.004
FedAvg	0.795±0.007	<u>0.812±0.006</u>	0.812±0.002	<u>0.780±0.008</u>	<u>0.782±0.008</u>
FedProx	0.791±0.006	<u>0.810±0.006</u>	0.811±0.003	<u>0.773±0.004</u>	<u>0.780±0.005</u>
FedBN	0.798±0.004	<u>0.815±0.007</u>	<u>0.815±0.002</u>	<u>0.780±0.008</u>	<u>0.785±0.006</u>
FedPxD	0.798±0.003	<u>0.813±0.006</u>	0.813±0.003	<u>0.777±0.009</u>	<u>0.783±0.004</u>
Centralized	0.809±0.004	0.823±0.001	0.823±0.004	0.782±0.012	0.792±0.008

Table 1: Average macro AUROC results across 12 clinical tasks for MIMIC-III-CV, MIMIC-III-MV, MIMIC-IV, eICU-South, eICU-West. All five clients are involved for federated learning and centralized learning. Underlined values indicate federated learning performance higher than single-source performance.

of our knowledge, our framework is the first to enable federated learning with clients of distinct medical codes and EHR database schemas.

Table 1 shows the average macro AUROC results across 12 clinical tasks on three distinct scenarios: federated learning on our EHRFL framework, single-source modeling trained on each client’s data, and centralized learning with aggregated data from all clients. We include single-source and centralized training results for comparison with our EHRFL outcomes. Single-source training results indicate the performance attainable from solely training on an individual client’s data, considered as a lower-bound. Conversely, centralized learning shows the results achievable by training on aggregated data across multiple data sources, representing an optimal scenario. Each client’s dataset is partitioned into train, validation, and test sets in an 8:1:1 ratio.

The results show that the federated learning performance for each client is either comparable to or higher than single-source results. In cases where federated learning performance is comparable but not higher than single-source performance (i.e., MIMIC-III-CV, MIMIC-IV), the results underscore the ongoing challenge of addressing the non-IID problem in existing current federated learning algorithms (e.g., FedProx, FedBN, FedPxD), despite their focus on mitigating the non-IID issue, particularly when compared to the centralized learning performance. However, notably, the federated learning performance higher than that of single-source modeling for certain clients (i.e., MIMIC-III-MV, eICU-South, and eICU-West) highlights the capability of our framework to facilitate collaborative learning across data sources of heterogeneous EHR systems. These results provide the first empirical evidence of the feasibility and effectiveness of federated learning across heterogeneous EHR systems.

In Section 5.5, we further apply our precision-based method outlined in Section 4 for selecting participating clients, aiming for reducing clients for cost reduction of the host.

#### 5.4. Correlation between Precision and Model Performance

In this section, we investigate the relationship between precision (alongside recall) of each host-subject pair and the model performance difference, in which performance difference is

Host Size	Metric	Correlation	Subject Size			
			4k	8k	12k	16k
4k	Precision	Spearman	0.441	0.49	0.517	0.533
		Kendall	0.289	0.333	0.365	0.397
4k	Recall	Spearman	-0.145	-0.107	0.067	0.138
		Kendall	-0.081	-0.071	0.064	0.109
8k	Precision	Spearman	0.505	0.519	0.622	0.679
		Kendall	0.358	0.334	0.421	0.477
8k	Recall	Spearman	0.148	0.191	0.319	0.402
		Kendall	0.098	0.128	0.218	0.275
12k	Precision	Spearman	0.409	0.605	0.557	0.517
		Kendall	0.284	0.409	0.371	0.348
12k	Recall	Spearman	0.119	0.326	0.219	0.164
		Kendall	0.083	0.224	0.147	0.107
16k	Precision	Spearman	0.262	0.366	0.434	0.511
		Kendall	0.176	0.232	0.286	0.349
16k	Recall	Spearman	0.134	0.168	0.318	0.228
		Kendall	0.093	0.099	0.221	0.172

Table 2: Correlation between precision (and recall) with performance delta in two-client federated learning scenarios. Each correlation value is derived from 60 data points, representing 20 host-subject combinations across three seeds.

measured between the host’s performance in federated learning when a specific subject is involved compared to the performance of a single-source model by the host. Subsequently, we refer to this difference as *performance delta*. If a positive correlation exists between the two, it would provide grounds for excluding clients with low precision scores, who may otherwise negligibly or negatively impact model performance. Our experiments are conducted in two-client settings (i.e., one host and one subject), representing the minimal client configuration in federated learning.

To measure correlations across diverse federated learning settings, we construct clients of multiple cohort sizes. Specifically, subsets of 4k, 8k, 12k, and 16k are sampled to construct training sets, from each of MIMIC-III-CV, MIMIC-III-MV, MIMIC-IV, eICU-South, and eICU-West datasets, resulting in a total of 20 clients. For each client, validation and test sets are sampled to include 2k each. We experiment across all possible combinations of host-subject pairs to comprehensively assess the impact of precision (and recall) on federated learning.

Precision (and recall) between the host and each subject are computed with the steps described in Section 4, using latent representations. With the precision (and recall) values of each host-subject pair, we measure the correlation between the precision (and recall) and performance delta. Table 2 shows the overall correlations.

The results indicate that across all host-subject pairs of different size combinations, the average correlation between precision and performance delta is 0.498 (standard deviation 0.101) for Spearman’s rank and 0.339 (standard deviation 0.074) for Kendall’s tau. Additionally, the correlation between recall and performance delta averages to 0.168 (standard deviation 0.146) for Spearman’s rank and 0.118 (standard deviation 0.097) for Kendall’s tau.

The correlations for precision were high and consistent, while correlations for recall were relatively low and showed higher standard deviations. The correlation levels for precision indicate a positive relationship between precision and performance delta in the two-client federated learning settings. We additionally measured the correlation in multiple client federated learning scenarios, in order to confirm the relevance of precision and performance not only in two-client settings but also in multiple client settings. The results are detailed in Appendix D.

### 5.5. Selecting Participating Clients for Federated Learning

As discussed earlier, increased number of clients in federated learning incurs elevated costs for the host. Therefore, it is crucial to optimize client participation by excluding clients that may potentially contribute minimally or detrimentally to the host’s performance. In this section, we investigate the feasibility of maintaining federated learning performance with fewer participating clients, specifically when appropriate clients are selected. Furthermore, we employ our precision-based method for selecting participating clients, and compare it’s efficacy against other baseline metrics of measuring client distance.

Table 3 presents the federated learning results for each host based on the total number of participating clients, with clients selected using our precision-based method and other baseline metrics (i.e., cosine similarity, euclidean distance, and KL-divergence). Cosine similarity and euclidean distance are computed as the averaged patient-wise similarity and distance using the host and subject patient latent vectors, aligned to that of Elhussein and Gürsoy (2023) and Huang et al. (2019), respectively. KL-divergence is measured between the softmax-normalized latent vectors of the host and subject. When selecting participating clients, we exclude the top clients with lowest precision scores for precision-based selection and the top clients with furthest distance values for the other baseline metrics respectively. Additionally, we perform federated learning across all possible client combinations, and present the *random* and *best* performance. *Random* indicates the average performance across all combinations, implying the performance achievable when participating clients are randomly selected, and *best* indicates the highest performance obtained, indicating the upper-bound performance. The precision scores for each host-subject pair are depicted in Figure 3.

The results show that in 14 out of 15 cases (across 3 client count settings with 5 clients each), the *best* performance with reduced number of participating clients aligns with that of when all clients are involved (i.e., 5-client performance). Such results demonstrate that in some cases, reducing the number of participants without compromising model performance is possible, which underscores the need for selecting participating clients. Notably, among the 14 cases where *best* performance aligns with the full client participation performance, there are 11 cases in which the *random* performance is lower than and does not align with the full client performance. Such results highlights the importance of carefully selecting suitable clients for the host.

In evaluating the number of cases where client-selected performance aligns with the *best* performance, the results from employing precision, cosine similarity, euclidean distance, and KL-divergence for selection each results in 9, 3, 6, and 5 aligned cases respectively. This indicates that our precision-based method outperforms other baseline metrics in aligning

# Clients	Metric	MIMIC-III-CV	MIMIC-III-MV	MIMIC-IV	eICU-South	eICU-West
2	Cosine	0.791	0.802	<b>0.814*</b>	0.771	0.777
	Euclidean	0.794	0.811*	<b>0.814*</b>	0.774	0.775
	KL	0.794	0.811*	<b>0.814*</b>	0.774	0.775
	<b>Precision</b>	<b>0.799*</b>	0.810	<b>0.814*</b>	<b>0.778*</b>	<b>0.784*</b>
	Random	0.792	0.806	<b>0.813</b>	0.774	0.779
	Best	<b>0.799</b>	0.811	<b>0.814</b>	<b>0.778</b>	<b>0.784</b>
3	Cosine	0.789	0.801	0.811	<b>0.778*</b>	0.779
	Euclidean	<b>0.799*</b>	<b>0.813*</b>	<b>0.814</b>	0.775	0.777
	KL	<b>0.799*</b>	<b>0.813*</b>	<b>0.814</b>	0.775	0.777
	<b>Precision</b>	<b>0.799*</b>	<b>0.813*</b>	<b>0.814</b>	<b>0.777</b>	<b>0.783</b>
	Random	0.794	0.808	0.812	0.776	0.781
	Best	<b>0.799</b>	<b>0.813</b>	<b>0.815</b>	<b>0.778</b>	<b>0.785</b>
4	Cosine	0.795	0.809	0.810	<b>0.778*</b>	<b>0.783</b>
	Euclidean	<b>0.796</b>	<b>0.814*</b>	0.812	0.776	<b>0.787*</b>
	KL	<b>0.796</b>	<b>0.814*</b>	0.812	0.776	0.778
	<b>Precision</b>	<b>0.796</b>	<b>0.814*</b>	<b>0.813</b>	<b>0.778*</b>	<b>0.787*</b>
	Random	0.794	0.811	<b>0.813</b>	0.777	<b>0.783</b>
	Best	<b>0.797</b>	<b>0.814</b>	<b>0.816</b>	<b>0.778</b>	<b>0.787</b>
5	-	0.796	0.813	0.813	0.777	0.782

Table 3: Federated Learning performance using our precision-based method and three baselines for selecting participating clients. Results are derived from the average of three seeds and present the mean macro AUROC across 12 clinical tasks. The results are averaged across the four federated learning algorithms, FedAvg, FedProx, FedBN, and FedPxD. Bold values indicate instances where the performance aligns with full client participation (i.e., 5 clients) performance. Asterisk indicates instances where the metric performance aligns with *best* performance.

with the upper-bound performance, highlighting the efficacy of our method in selecting appropriate participating clients for the host. Furthermore, when selecting participating clients with our precision-based method, 14 out of 15 cases achieve equal or higher performance compared to the full client participation performance. Such results suggest that our precision-based method can maintain the performance achieved with full client engagement while reducing the number of participating clients.

To ensure the robustness of our precision-based method across different datasets, we construct a new set of clients and compare the federated learning results when clients are selected using our precision-based method and the other baselines. The results, detailed in Appendix E, consistently corroborate our analysis for observations in Table 3, confirming the necessity of client selection and the effectiveness of our precision-based method.

## 6. Discussion and Conclusion

In this study, we provide solutions to two realistic yet underexplored scenarios in EHR federated learning. We first introduce the Electronic Health Record Federated Learning framework (EHRFL), which facilitates federated learning across healthcare institutions with heterogeneous electronic health record systems by utilizing text-based EHR linearization. Furthermore, we propose a novel precision-based method, which leverages data latents to select participating clients by identifying clients to exclude, in the perspective of a single healthcare institution. Our experiment results demonstrate, for the first time, the feasibility and effectiveness of federated learning on distinct EHR systems by using our EHRFL framework. Additionally, we empirically show that in some cases maintaining federated learning performance with fewer participating clients is possible, particularly when suitable clients for the host are selected, highlighting the necessity of selecting participating clients. Furthermore, our experiments validate the efficacy of our precision-based method in identifying and excluding non-ideal clients, thereby optimizing the number of participants without compromising model performance for the host. We believe this research provides a foundation for expanding the practical implementation of federated learning in healthcare.

### Limitations

Although our EHRFL framework demonstrates performance improvements in federated learning compared to single-source models, we do not directly compare our results with those obtained through federated learning after mapping to a standardized format such as Common Data Model (CDM) (Rajkomar et al., 2018; Biedermann et al., 2021). CDMs utilize predefined schemas and medical terminologies to store EHRs from various healthcare institutions in a unified format. While the conversion of EHRs into CDM format can be labor-intensive and costly, future research can provide insights in how our framework, without schema and code mapping, compares in performance to those using standardized formats such as CDMs for federated learning.

While our experimental findings underscore the efficacy of our precision-based method in optimizing client participation through selective exclusion, determining the optimal number of participating clients remains an area of further study. We believe that identifying the optimal client count can further enhance the applicability of our method in federated learning for EHRs.

### References

- Ali Amirahmadi, Mattias Ohlsson, and Kobra Etminani. Deep learning prediction models based on ehr trajectories: A systematic review. *Journal of Biomedical Informatics*, page 104430, 2023.
- Patricia Biedermann, Rose Ong, Alexander Davydov, Alexandra Orlova, Philip Solovyev, Hong Sun, Graham Wetherill, Monika Brand, and Eva-Maria Didden. Standardizing registry data to the omop common data model: experience from three pulmonary hypertension databases. *BMC medical research methodology*, 21:1–16, 2021.

- Edward Choi, Mohammad Taha Bahadori, Andy Schuetz, Walter F Stewart, and Jimeng Sun. Doctor ai: Predicting clinical events via recurrent neural networks. In *Machine learning for healthcare conference*, pages 301–318. PMLR, 2016.
- Trung Kien Dang, Xiang Lan, Jianshu Weng, and Mengling Feng. Federated learning for electronic health records. *ACM Transactions on Intelligent Systems and Technology (TIST)*, 13(5):1–17, 2022.
- Sabyasachi Dash, Sushil Kumar Shakyawar, Mohit Sharma, and Sandeep Kaushik. Big data in healthcare: management, analysis and future prospects. *Journal of big data*, 6(1):1–25, 2019.
- Ahmed Elhoussein and Gamze Gürsoy. Privacy-preserving patient clustering for personalized federated learnings. In *Machine Learning for Healthcare Conference*, pages 150–166. PMLR, 2023.
- Li Huang, Andrew L Shea, Huining Qian, Aditya Masurkar, Hao Deng, and Dianbo Liu. Patient clustering improves efficiency of federated machine learning to predict mortality and hospital stay time using distributed electronic medical records. *Journal of biomedical informatics*, 99:103291, 2019.
- Kyunghoon Hur, Jungwoo Oh, Junu Kim, Jiyoung Kim, Min Jae Lee, Eunbyeol Cho, Seong-Eun Moon, Young-Hak Kim, Louis Atallah, and Edward Choi. Genhpf: General healthcare predictive framework for multi-task multi-source learning. *IEEE Journal of Biomedical and Health Informatics*, 2023.
- Hyeonji Hwang, Seongjun Yang, Daeyoung Kim, Radhika Dua, Jong-Yeup Kim, Eunho Yang, and Edward Choi. Towards the practical utility of federated learning in the medical domain. In *Conference on Health, Inference, and Learning*, pages 163–181. PMLR, 2023.
- Alistair Johnson, Lucas Bulgarelli, Tom Pollard, Steven Horng, Leo Anthony Celi, and Roger Mark. Mimic-iv. *PhysioNet*. Available online at: <https://physionet.org/content/mimiciv/1.0/>(accessed August 23, 2021), 2020.
- Alistair EW Johnson, Tom J Pollard, Lu Shen, Li-wei H Lehman, Mengling Feng, Mohammad Ghassemi, Benjamin Moody, Peter Szolovits, Leo Anthony Celi, and Roger G Mark. Mimic-iii, a freely accessible critical care database. *Scientific data*, 3(1):1–9, 2016.
- Tuomas Kynkäänniemi, Tero Karras, Samuli Laine, Jaakko Lehtinen, and Timo Aila. Improved precision and recall metric for assessing generative models. *Advances in Neural Information Processing Systems*, 32, 2019.
- Geun Hyeong Lee and Soo-Yong Shin. Federated learning on clinical benchmark data: performance assessment. *Journal of medical Internet research*, 22(10):e20891, 2020.
- Qinbin Li, Yiqun Diao, Quan Chen, and Bingsheng He. Federated learning on non-iid data silos: An experimental study. In *2022 IEEE 38th international conference on data engineering (ICDE)*, pages 965–978. IEEE, 2022.

- Tian Li, Anit Kumar Sahu, Manzil Zaheer, Maziar Sanjabi, Ameet Talwalkar, and Virginia Smith. Federated optimization in heterogeneous networks. *Proceedings of Machine learning and systems*, 2:429–450, 2020.
- Xiaoxiao Li, Meirui Jiang, Xiaofei Zhang, Michael Kamp, and Qi Dou. Fedbn: Federated learning on non-iid features via local batch normalization. *arXiv preprint arXiv:2102.07623*, 2021.
- Ibrahim Abdul Majeed, Hwang-Ki Min, Venkata Siva Kumar Tadi, Sagar Kaushik, Anirudha Bardhan, Karthikeyan Kumaraguru, and Rajasekhara Reddy Duvvuru Muni. Factors influencing cost and performance of federated and centralized machine learning. In *2022 IEEE 19th India Council International Conference (INDICON)*, pages 1–6. IEEE, 2022.
- Brendan McMahan, Eider Moore, Daniel Ramage, Seth Hampson, and Blaise Aguera y Arcas. Communication-efficient learning of deep networks from decentralized data. In *Artificial intelligence and statistics*, pages 1273–1282. PMLR, 2017.
- Tom J Pollard, Alistair EW Johnson, Jesse D Raffa, Leo A Celi, Roger G Mark, and Omar Badawi. The eicu collaborative research database, a freely available multi-center database for critical care research. *Scientific data*, 5(1):1–13, 2018.
- Anichur Rahman, Md Sazzad Hossain, Ghulam Muhammad, Dipanjali Kundu, Tanoy Deb-nath, Muaz Rahman, Md Saikat Islam Khan, Prayag Tiwari, and Shahab S Band. Federated learning-based ai approaches in smart healthcare: concepts, taxonomies, challenges and open issues. *Cluster computing*, 26(4):2271–2311, 2023.
- Suraj Rajendran, Zhenxing Xu, Weishen Pan, Arnab Ghosh, and Fei Wang. Data heterogeneity in federated learning with electronic health records: Case studies of risk prediction for acute kidney injury and sepsis diseases in critical care. *PLOS Digital Health*, 2(3):e0000117, 2023.
- Alvin Rajkomar, Eyal Oren, Kai Chen, Andrew M Dai, Nissan Hajaj, Michaela Hardt, Peter J Liu, Xiaobing Liu, Jake Marcus, Mimi Sun, et al. Scalable and accurate deep learning with electronic health records. *NPJ digital medicine*, 1(1):18, 2018.
- Nicola Rieke, Jonny Hancox, Wenqi Li, Fausto Milletari, Holger R Roth, Shadi Albarqouni, Spyridon Bakas, Mathieu N Galtier, Bennett A Landman, Klaus Maier-Hein, et al. The future of digital health with federated learning. *NPJ digital medicine*, 3(1):119, 2020.
- Akhil Vaid, Suraj K Jaladanki, Jie Xu, Shelly Teng, Arvind Kumar, Samuel Lee, Sulaiman Somani, Ishan Paranjpe, Jessica K De Freitas, Tingyi Wanyan, et al. Federated learning of electronic health records to improve mortality prediction in hospitalized patients with covid-19: machine learning approach. *JMIR medical informatics*, 9(1):e24207, 2021.
- Ashish Vaswani, Noam Shazeer, Niki Parmar, Jakob Uszkoreit, Llion Jones, Aidan N Gomez, Lukasz Kaiser, and Illia Polosukhin. Attention is all you need. *Advances in neural information processing systems*, 30, 2017.



Jie Wen, Zhixia Zhang, Yang Lan, Zhihua Cui, Jianghui Cai, and Wensheng Zhang. A survey on federated learning: challenges and applications. *International Journal of Machine Learning and Cybernetics*, 14(2):513–535, 2023.

Xi Yang, Aokun Chen, Nima PourNejatian, Hoo Chang Shin, Kaleb E Smith, Christopher Parisien, Colin Compas, Cheryl Martin, Anthony B Costa, Mona G Flores, et al. A large language model for electronic health records. *NPJ Digital Medicine*, 5(1):194, 2022.

Chen Zhang, Yu Xie, Hang Bai, Bin Yu, Weihong Li, and Yuan Gao. A survey on federated learning. *Knowledge-Based Systems*, 216:106775, 2021.

## Appendix A. Definition of Predictive Tasks

We adopted 12 clinical predictive tasks from [Hur et al. \(2023\)](#). The tasks aim to predict various clinical events within the next 24 hours, based on data from the first 12 hours of a patient’s ICU admission, unless otherwise specified. Descriptions of each task are detailed as follows:

- **Mortality Prediction (Mort, Binary):** Predicts whether the patient dies within the next 24 hours.
- **Two-Week Mortality Prediction (Mort\_2w, Binary):** Predicts whether the patient dies within the next two weeks.
- **Three-Day ICU Stay Prediction (LOS\_3day, Binary):** Predicts whether the ICU stay is longer than three days.
- **Seven-Day ICU Stay Prediction (LOS\_7day, Binary):** Predicts whether the ICU stay is longer than seven days.
- **ICU Readmission Prediction (Readm, Binary):** Predicts whether the patient will be readmitted to the ICU within the same hospital admission.
- **Bilirubin Level Prediction (Bilirubin, Multi-Class):** Predicts the future serum bilirubin levels, classified into five classes.
- **Creatinine Level Prediction (Creatinine, Multi-Class):** Predicts the future serum creatinine levels, classified into five classes.
- **Discharge Acuity Prediction (Final\_Acuity, Multi-Class):** Predicts the patient’s discharge location at the end of the hospital stay.
- **Imminent Discharge Prediction (Im\_Disch, Multi-Class):** Predicts whether the patient will be discharged within the next 24 hours and predicts the discharge location.
- **Platelet Count Prediction (Platelets, Multi-Class):** Predicts the future platelet counts, categorized into five classes.
- **White Blood Cell Count Prediction (WBC, Multi-Class):** Predicts the future white blood cell counts, classified into three classes.
- **Diagnosis Prediction (Diagnosis, Multi-Label):** Predicts all diagnosis codes of the patient’s admission, classified into 18 classes.

## Appendix B. Client Statistics

		MIMICIII-CV	MIMIC-III-MV	MIMIC-IV	eICU-South	eICU-West
Cohort Size		24,710	20,288	34,888	45,379	27,656
Gender (%)	Male	56.5	55.8	55.8	53.1	54.9
	Female	43.5	44.2	44.2	46.9	45.1
Ethnicity (%)	White	70.6	72.8	66.0	68.5	77.2
	Black	8.7	10.6	10.9	21.0	4.6
	Hispanic	2.9	4.1	3.6	5.4	4.9
	Asian	2.0	2.7	3.1	1.1	3.2
	Others	15.8	9.8	16.4	4.0	10.1

Table 4: Demographic Information of the five clients in Section 5.3 and Section 5.5.

		eICU-73	eICU-264	eICU-420	eICU-338	eICU-300
Cohort Size		5234	4383	3760	3478	3050
Gender (%)	Male	54.39	51.70	57.34	55.98	54.72
	Female	45.61	48.30	42.55	44.02	45.28
Ethnicity (%)	White	75.63	90.00	85.90	93.15	85.18
	Black	15.14	7.43	4.20	1.50	10.56
	Hispanic	7.37	0.35	0.11	1.41	0.85
	Asian	1.30	0.77	1.49	0.20	0.89
	Others	0.56	1.45	8.40	3.74	2.53

Table 5: Demographic Information of the five clients in Appendix E.

EHRFL

Type	Task	Label	Distributions (%)				
			MIMIC-III-CV	MIMIC-III-MV	MIMIC-IV	eICU-South	eICU-West
Binary	Mort	True	1.8	1.6	1.6	1.8	1.8
	Mort_2w	True	9.0	7.7	7.8	7.9	7.3
	LOS_3day	True	36.7	30.9	29.9	29.9	25.5
	LOS_7day	True	13.4	10.5	9.0	9.1	7.9
	Readm	True	5.4	5.6	7.3	8.7	14.6
Multi-Class	Bilirubin	0	12.0	14.7	18.1	17.5	26.8
		1	2.7	3.0	3.7	2.7	4.2
		2	3.1	4.2	4.1	2.1	3.3
		3	0.9	1.2	1.1	0.4	0.6
		4	0.8	0.8	0.9	0.2	0.5
	Creatinine	0	60.0	58.1	58.9	47.6	50.8
		1	16.0	16.2	16.5	15.6	13.4
		2	6.2	6.1	6.5	7.2	5.9
		3	1.6	1.5	1.8	2.5	1.8
		4	1.4	1.3	1.8	2.7	2.0
	Final Acuity	0	52.3	51.5	52.5	61.2	61.1
		1	3.6	3.1	3.8	3.9	3.1
		2	7.8	6.4	6.1	5.3	5.3
		3	6.7	13.2	10.6	15.4	12.1
		4	15.7	8.4	6.7	4.6	1.9
		5	13.9	17.5	19.5	9.1	15.3
	Im_Disch	0	1.8	1.6	1.6	1.8	1.8
		1	1.9	2.6	2.8	4.9	5.6
		2	95.7	95.0	94.4	91.8	90.7
		3	0.4	0.7	0.5	1.3	1.7
4		0.1	0.0	0.0	0.0	0.0	
5		0.1	0.1	0.1	0.1	0.1	
Platelets	0	61.9	61.7	55.6	48.9	45.6	
	1	17.3	16.4	21.0	15.9	15.1	
	2	7.7	7.2	9.4	7.2	7.2	
	3	1.4	2.0	2.5	1.6	1.8	
	4	0.2	0.3	0.4	0.3	0.3	
WBC	0	3.1	4.3	3.5	2.6	2.4	
	1	51.1	55.9	54.1	44.4	43.8	
	2	33.8	27.2	31.3	26.9	26.9	
	3	26.1	33.6	38.4	10.4	18.1	
Multi-Label Diagnosis	1	22.6	31.1	32.1	6.0	5.4	
	2	65.3	78.0	83.1	31.4	24.1	
	3	33.0	46.3	57.6	13.2	7.8	
	4	28.2	48.0	68.8	11.0	10.8	
	5	23.0	41.6	52.0	15.6	14.6	
	6	82.5	85.8	89.2	57.6	51.1	
	7	48.2	52.7	54.7	34.2	32.9	
	8	39.8	53.3	58.6	14.6	14.0	
	9	39.9	52.1	55.6	22.4	18.1	
	10	0.4	0.4	0.6	0.6	0.4	
	11	9.8	12.0	11.8	1.4	1.8	
	12	16.0	31.5	35.3	1.6	1.6	
	13	3.0	3.9	5.1	0.1	0.0	
	14	43.7	46.3	43.2	13.8	13.7	
	15	20.2	39.4	59.5	13.0	11.7	
	16	33.1	59.4	75.7	7.2	3.9	

Table 6: Label distributions of the five clients in Section 5.3 and Section 5.5 on 12 tasks.

EHRFL

Type	Task	Label	Distributions (%)				
			eICU-73	eICU-264	eICU-420	eICU-338	eICU-300
Binary	Mort	True	1.03	1.87	1.81	1.52	0.95
	Mort_2w	True	5.43	7.87	10.24	6.38	6.39
	LOS_3day	True	30.99	36.66	42.34	30.74	30.56
	LOS_7day	True	9.34	10.70	14.89	9.40	10.82
	Readm	True	16.22	6.41	11.41	7.94	6.26
Multi-Class	Bilirubin	0	19.53	9.77	11.30	24.35	20.20
		1	2.98	1.55	2.39	3.34	2.23
		2	2.67	1.69	3.38	2.56	2.13
		3	0.63	0.57	0.80	0.40	0.49
		4	0.31	0.14	0.69	0.12	0.13
	Creatinine	0	42.17	54.46	56.33	52.44	54.33
		1	19.18	13.16	14.97	14.00	14.30
		2	7.34	6.23	6.76	5.00	5.25
		3	3.02	2.14	1.73	1.12	1.31
		4	3.46	2.03	1.49	0.78	1.44
	Final Acuity	0	66.07	55.74	47.77	60.67	56.13
		1	5.22	3.86	3.62	2.39	3.02
		2	1.43	4.84	8.48	5.20	5.08
		3	6.99	7.21	5.61	11.18	10.56
		4	6.25	5.02	20.48	5.38	9.93
	Im_Disch	0	1.03	1.87	1.81	1.78	1.11
		1	4.30	4.68	2.61	2.76	4.72
		2	94.08	92.36	94.41	94.65	92.66
		3	0.46	0.84	0.74	0.69	1.41
		4	0.00	0.05	0.16	0.03	0.00
Platelets	0	55.25	56.97	54.36	46.78	51.02	
	1	17.60	13.64	20.19	15.96	16.75	
	2	7.72	5.54	10.03	7.85	6.43	
	3	1.55	1.19	2.45	1.50	1.44	
	4	0.29	0.25	0.59	0.37	0.33	
WBC	0	3.02	2.49	3.19	2.76	2.79	
	1	51.09	47.57	52.47	43.65	48.13	
	2	27.89	27.77	31.70	26.14	25.05	
	3	14.00	14.00	14.00	14.00	14.00	
Multi-Label	Diagnosis	0	9.23	6.55	24.18	0.81	0.98
		1	5.73	4.65	12.85	2.24	3.31
		2	23.73	8.65	93.16	11.16	10.20
		3	6.53	4.24	66.46	2.47	3.02
		4	6.42	5.20	73.43	3.34	3.80
		5	10.20	16.63	44.49	9.57	9.64
		6	45.95	43.08	89.20	42.67	37.67
		7	26.46	29.55	74.07	25.62	21.28
		8	8.88	12.23	43.86	8.88	8.23
		9	19.43	9.17	49.89	9.14	8.79
		10	0.27	0.11	0.29	0.03	0.13
		11	1.05	1.03	6.04	1.50	2.03
		12	1.15	1.57	5.13	0.98	1.74
		13	0.10	0.00	0.11	0.03	0.00
		14	11.77	11.11	48.27	12.39	19.02
		15	7.36	7.28	48.01	5.38	5.41
16	5.66	2.42	78.01	2.01	2.33		

Table 7: Label distributions the five clients in Appendix E on 12 tasks.

## Appendix C. Experimental Results

Dataset	Algorithm	Bilirubin	Creatinine	Diagnosis	Final_Acuity	Im_Disch	Mort_2w	LOS3	LOS7	Mort	Platelets	Readm	WBC	Average
MIMIC-III-CV	Single	0.847	0.951	0.810	0.829	0.993	0.854	0.762	0.799	0.910	0.949	0.639	0.857	0.800
	FedAvg	0.862	0.947	0.807	0.812	0.988	0.857	0.758	0.799	0.899	0.944	0.628	0.863	0.797
	FedProx	0.859	0.945	0.807	0.814	0.988	0.852	0.763	0.803	0.887	0.944	0.618	0.860	0.792
	FedBN	0.864	0.948	0.811	0.828	0.989	0.856	0.766	0.807	0.891	0.946	0.634	0.863	0.798
	FedPxN	0.861	0.947	0.810	0.830	0.989	0.855	0.768	0.810	0.900	0.947	0.638	0.860	0.798
	Centralized	0.868	0.948	0.813	0.832	0.993	0.860	0.772	0.808	0.915	0.947	0.648	0.857	0.809
MIMIC-III-MV	Single	0.827	0.946	0.800	0.829	0.992	0.860	0.783	0.816	0.931	0.947	0.629*	0.868	0.802
	FedAvg	0.854	0.948	0.805	0.834	0.989	0.883	0.797	0.836	0.944	0.945	0.661	0.868	0.813
	FedProx	0.854	0.945	0.805	0.834	0.988	0.881	0.793	0.832	0.948	0.944	0.646	0.864	0.811
	FedBN	0.854	0.948	0.808	0.836	0.990	0.884	0.800	0.840	0.952	0.948	0.671*	0.868	0.815
	FedPxN	0.854	0.946	0.809	0.840	0.988	0.882	0.795	0.836	0.953	0.947	0.663	0.870	0.813
	Centralized	0.857	0.948	0.811	0.839	0.993	0.891	0.806	0.839	0.953	0.947	0.666	0.868	0.823
MIMIC-IV	Single	0.879	0.953	0.837	0.841	0.991	0.870	0.745	0.798	0.924	0.944	0.633*	0.885	0.815
	FedAvg	0.872	0.949	0.821	0.836	0.987	0.880	0.769*	0.824	0.923	0.942	0.655	0.878	0.811
	FedProx	0.875	0.947	0.820	0.841	0.987	0.882	0.765	0.822	0.930	0.942	0.646	0.876	0.810
	FedBN	0.880	0.950	0.837	0.846	0.988	0.881	0.754	0.810	0.938	0.943	0.652	0.886	0.815
	FedPxN	0.879	0.950	0.837	0.846	0.988	0.878	0.752	0.808	0.932	0.943	0.657	0.886	0.813
	Centralized	0.883	0.950	0.842	0.844	0.992	0.879	0.756	0.813	0.944	0.942	0.653	0.885	0.823
eICU-South	Single	0.867	0.904	0.865	0.870	0.982	0.824	0.732	0.779	0.874	0.916	0.625	0.833	0.775
	FedAvg	0.873	0.910	0.866	0.863	0.975	0.837	0.739	0.788	0.890	0.916	0.623	0.838	0.780
	FedProx	0.873	0.908	0.863	0.862	0.975	0.838	0.735	0.786	0.887	0.915	0.618	0.837	0.773
	FedBN	0.872	0.908	0.867	0.867	0.976	0.836	0.739	0.787	0.886	0.915	0.625	0.836	0.780
	FedPxN	0.873	0.909	0.866	0.867	0.977	0.840	0.736	0.789	0.893	0.915	0.622	0.837	0.778
	Centralized	0.876	0.907	0.868	0.866	0.982	0.833	0.735	0.783	0.884	0.914	0.631	0.832	0.782
eICU-West	Single	0.872	0.916	0.874	0.866	0.976	0.810	0.743	0.765	0.871*	0.899	0.697	0.812	0.770
	FedAvg	0.881	0.919	0.871	0.856	0.969	0.840	0.746	0.776	0.889*	0.906	0.670	0.829	0.782
	FedProx	0.881	0.916	0.871	0.856	0.968	0.840	0.746	0.774	0.894*	0.906	0.661	0.826	0.780
	FedBN	0.882	0.921	0.877	0.864	0.968	0.841	0.753	0.782	0.889*	0.905	0.688	0.830	0.784
	FedPxN	0.882	0.918	0.877	0.865	0.969	0.842	0.752	0.778	0.893	0.906	0.680	0.826	0.783
	Centralized	0.887	0.920	0.880	0.867	0.977	0.855	0.760	0.782	0.901	0.906	0.693	0.823	0.792

Table 8: AUROC scores for each of the 12 tasks regarding Table 1. The results represent averaged scores obtained from experiments conducted on three seeds. Asterisk (\*) denotes standard deviation higher than 0.03.

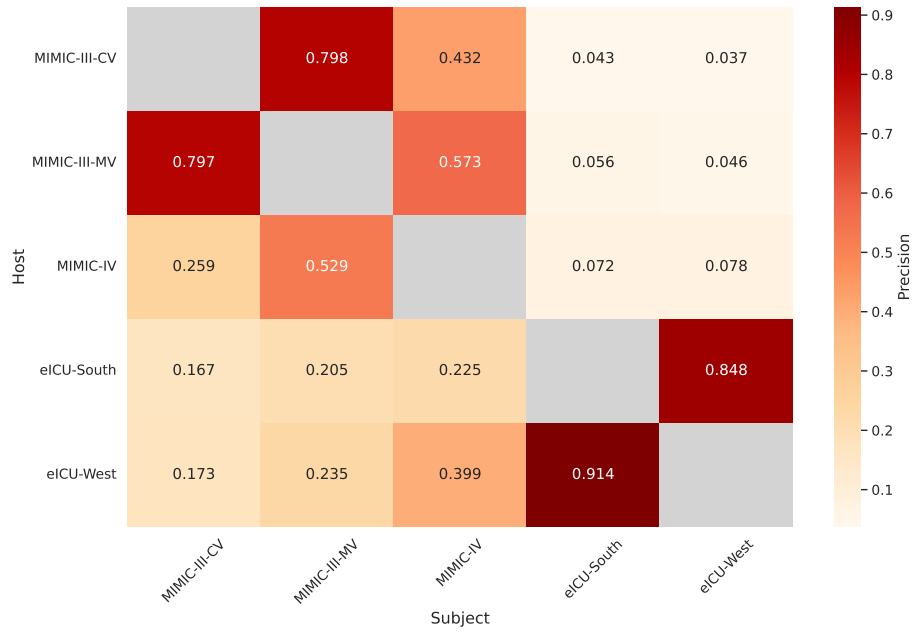


Figure 3: Precision Scores of each host-subject pair across MIMIC-III-CV, MIMIC-III-MV, MIMIC-IV, eICU-South, eICU-West. Precision is measured by sampling from the train data of each client based on the minimum train data size among the five clients. In our client setting, we sampled 16988 train data for each client, corresponding to the size of the smallest dataset, MIMIC-III-MV.

## Appendix D. Correlation between Precision and Performance Difference in Multi-client Scenarios

We measure the correlation between precision and performance difference across multiple client federated learning scenarios. We use the clients constructed in Section 5.4, which are characterized by varying sizes (i.e., 4k, 8k, 12k, and 16k), and varying data sources (i.e., MIMIC-III-CV, MIMIC-III-MV, MIMIC-IV, eICU-South, eICU-West). We experiment in a five-client setting, with each experiment consisting clients of identical sizes (either 4k, 8k, 12k, 16k). The core to this analysis is to compute the correlation between the precision of a given host-subject pair and the observed change in performance. This performance change is quantified as the difference in federated learning performance when engaging five clients in comparison to the results achieved with four clients, the latter scenario excluding the considered subject. Figure 4 shows the relationship between the precision associated with each subject and the observed performance drop from the perspective of each host. Across the four plots, consistent correlations were observed, averaging 0.339 (standard deviation 0.073) for Spearman’s rank, and 0.223 (standard deviation 0.057) for Kendall’s tau. Such results indicate a positive correlation between precision and performance increase, not only in two-client settings but also across multiple client settings.

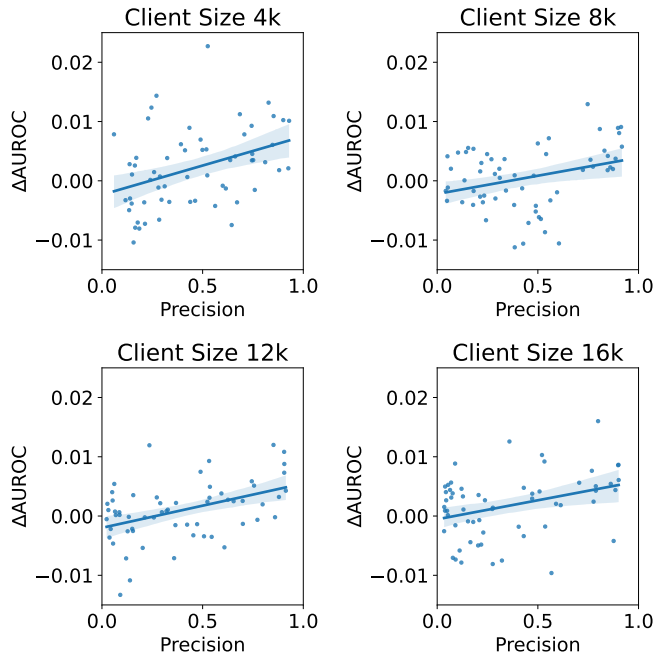


Figure 4: Visualization of precision and performance difference for multi-client federated learning scenarios. Each plot shows the 3-seed results of all possible pairings of host-subject of equal size. The x-axis quantifies the precision between the host and subject, while the y-axis measures the performance drop when five clients are involved in comparison to four client federated learning performance when the subject is excluded in the process. The shaded portion represents a 95% confidence interval.



## Appendix E. Selecting Participating Clients on Additional Datasets

This section evaluates our precision-based method on a newly constructed set of clients. We construct five distinct clients using the northeast and midwest regions of the eICU dataset, each client representing a different hospital: eICU-264, eICU-300, eICU-338, eICU-420, and eICU-73. The selection of data for each client follows the criteria outlined in Section 5.2, with the demographics and label distributions of each client listed in Appendix B.

Table 9 presents the federated learning results for each host based on the total number of participating clients, with clients selected using our precision-based method and other baseline metrics, with the metrics aligned to that elaborated in Section 5.5. The precision scores for each host-subject pair are depicted in Figure 5.

The results show that in 8 out of 15 cases (across 3 client count settings with 5 clients each), the *best* performance with reduced number of participating clients aligns with that of when all clients are involved (i.e., 5-client performance). Such results demonstrate that in some cases, reducing the number of participants without compromising model performance is possible, which underscores the need for selecting participating clients. Notably, among the 8 cases where *best* performance aligns with the full client participation performance, there are 5 cases in which the *random* performance is lower than and does not align with the full client performance. Such results highlights the importance of carefully selecting suitable clients for the host.

In evaluating the number of cases where client-selected performance aligns with the *best* performance, the results from employing precision, cosine similarity, euclidean distance, and KL-divergence for selection each results in 5, 4, 3 and 2 aligned cases respectively. This indicates that our precision-based method outperforms other baseline metrics in aligning with the upper-bound performance, highlighting the efficacy of our method in selecting appropriate participating clients for the host. Furthermore, when selecting participating clients with our precision-based method, 6 out of 15 cases achieve equal or higher performance compared to the full client participation performance. Such results suggests that our precision-based method can maintain the performance achieved with full client engagement while reducing the number of participating clients.

# Clients	Metric	eICU-73	eICU-420	eICU-338	eICU-300	eICU-264
2	Cosine	0.712	0.731	0.697	0.714	0.727
	Euclidean	0.703	<b>0.749*</b>	0.691	0.712	<b>0.745</b>
	KL	0.703	<b>0.749*</b>	0.700	0.712	<b>0.745</b>
	<b>Precision</b>	0.707	0.731	0.697	0.714	<b>0.745</b>
	Random	0.712	<b>0.741</b>	0.698	0.722	<b>0.739</b>
	Best	0.726	<b>0.749</b>	0.705	<b>0.743</b>	<b>0.755</b>
3	Cosine	0.724	<b>0.741</b>	0.716*	0.741*	0.736
	Euclidean	0.729	<b>0.740</b>	0.693	0.737	<b>0.752*</b>
	KL	0.712	<b>0.740</b>	0.693	0.737	<b>0.746</b>
	<b>Precision</b>	0.729	<b>0.741</b>	0.716*	0.741*	<b>0.746</b>
	Random	0.722	<b>0.743</b>	0.708	0.734	0.737
	Best	0.732	<b>0.752</b>	0.716	0.741	<b>0.752</b>
4	Cosine	0.729	<b>0.743*</b>	0.718*	0.736	0.738
	Euclidean	0.726	0.722	0.712	0.736	<b>0.753*</b>
	KL	0.726	0.722	0.712	0.736	<b>0.753*</b>
	<b>Precision</b>	0.726	<b>0.743*</b>	0.717	<b>0.748*</b>	<b>0.753*</b>
	Random	0.726	0.732	0.712	0.733	0.738
	Best	0.730	<b>0.743</b>	0.718	<b>0.748</b>	<b>0.753</b>
5	-	0.737	0.738	0.720	0.742	0.739

Table 9: Federated Learning performance using our precision-based method and three baselines for selecting participating clients. Results are derived from the average of three seeds and present the mean macro AUROC across 12 clinical tasks. The results are averaged across the four federated learning algorithms, FedAvg, FedProx, FedBN, and FedPxN. Bold values indicate instances where the performance aligns with full client participation (i.e., 5 clients) performance. Asterisk indicates instances where the metric performance aligns with *best* performance.

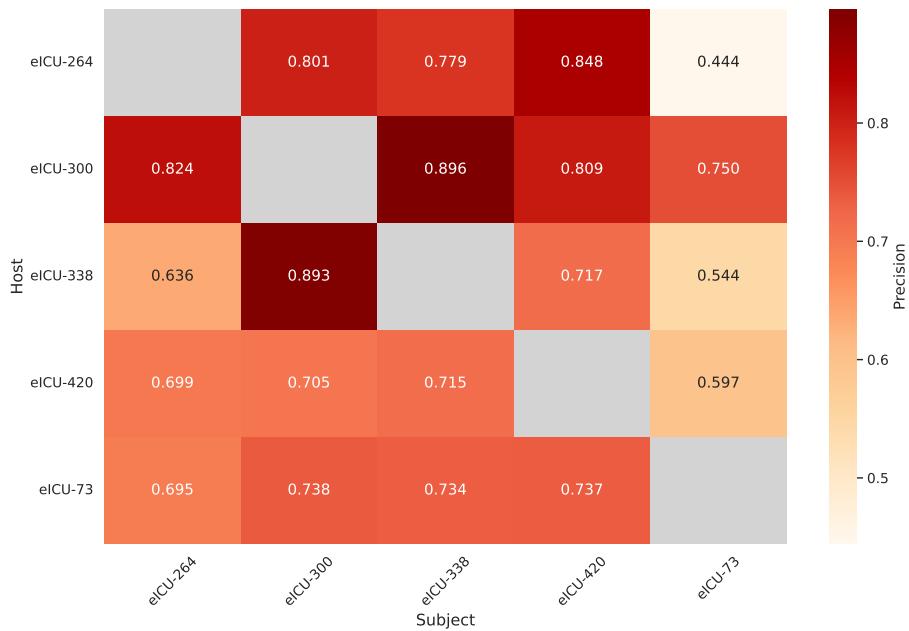


Figure 5: Precision Scores of each host-subject pair across eICU-264, eICU-300, eICU-338, eICU-420, eICU-73. Precision is measured by sampling from the train data of each client based on the minimum train data size among the five clients. In our client setting, we sampled 2440 train data for each client, corresponding to the size of the smallest dataset, eICU-300.